Journal of Physics and Chemistry of Solids 71 (2010) 235–241

Contents lists available at ScienceDirect

Journal of Physics and Chemistry of Solids

journal homepage: www.elsevier.com/locate/jpcs

Controllable synthesis and modification of carbon micro-spheres from deoiled asphalt

Yongzhen Yang [a,b], Xuguang Liu [a,c,*], Chun Yi Zhang [a,b], Mingcong Guo [a,c], Bingshe Xu [a,b]

[a] Key Laboratory of Interface Science and Engineering in Advanced Materials, Taiyuan University of Technology, Ministry of Education, Taiyuan 030024, China
[b] College of Materials Science and Engineering, Taiyuan University of Technology, Taiyuan 030024, China
[c] College of Chemistry and Chemical Engineering, Taiyuan University of Technology, Taiyuan 030024, China

ARTICLE INFO

Article history:
Received 10 February 2009
Received in revised form
25 November 2009
Accepted 26 November 2009

Keywords:
A. Amorphous materials
B. Vapour deposition
D. Microstructure
D. Surface properties

ABSTRACT

A series of size-controllable carbon micro-spheres (CMSs) were synthesized from deoiled asphalt by chemical vapour deposition, with the emphasis on the effect of reaction temperature, Ar flow rate and collection zone. Graphitized carbon micro-spheres (GCMSs) were obtained from as-prepared CMSs by vacuum heat treatment at 2000 °C for 1 h. Air oxidation was performed to realize functionalization of CMSs. Morphologies and structures of CMSs and GCMSs were characterized by field emission scanning electron microscopy, high-resolution transmission electron microscopy, energy dispersive X-ray spectroscopy, X-ray diffraction and Raman spectroscopy, and the functional groups on the surface of GCMSs and CMSs were characterized by Fourier transformation infra-red spectrometry. Results show that effective mass production of size-controllable CMSs, with diameters ranging from 100 nm to 1 μm, was achieved. As-obtained high purity CMSs were spherical with uniform size and low graphitization degree, but the graphitization degree of GCMSs was enhanced obviously. By air oxidation, some oxygen-containing functional groups were introduced onto the surface of CMSs, while no functional groups were introduced onto the surface of GCMSs.

1. Introduction

In 1990s, some scientists, such as Ugarte [1] and Iijima [2], brought the research of carbon materials to a new stage. Among various forms of carbon, carbon micro-spheres (CMSs) as a kind of advanced material are becoming increasingly important because of their special properties. Many potential applications for CMSs have been proposed, including anode material of secondary lithium ion batteries, catalyst supporter, fillers in composite and porous conductive material [3–6]. Up to now, various methods have been demonstrated for the synthesis of CMSs, such as emulsion, suspension, arc discharge, pressurized carbonization, chemical vapour deposition (CVD), etc. [7–13]. CVD is considered to be a suitable route for the synthesis of CMSs due to its simple technological operation and low cost. But the graphitization degree of CMSs synthesized by CVD is low. However, to expand and optimize the use of CMSs in research field, it is necessary to modify and functionalize their surface. The modification of CMSs is an essential step to graft a wide variety of functional groups or active molecules to their surface, or to improve their solubility either in common organic solvents or in aqueous solution. Deoiled asphalt (DOA) is a kind of carbon-rich by-product of petroleum processing. Converting DOA into carbon materials with high added value is an economically competent route [14–19]. The purpose of this work is to synthesize a series of size-controllable CMSs from DOA by CVD, and obtain graphitized carbon micro-spheres (GCMSs) from as-prepared CMSs by vacuum heat treatment, and then modify their surface by air oxidation.

2. Experimental

2.1. Synthesis of CMSs

DOA used in this experiment was supplied by China University of Petroleum-Beijing. Table 1 shows some analytical data of DOA, and Table 2 shows the main compositions of its pyrolytic gases.

Fig. 1 shows the schematic of experimental apparatus and the corresponding temperature profile along quartz tube reactor with the central temperature of 1100 °C. CMSs were synthesized in the quartz tube (32 mm i.d. and 1000 mm long), which was mounted in a horizontal tubular furnace. At the beginning of synthesis experiment, 2.0 g of DOA was placed in a small quartz boat located at the inlet cool zone of the quartz tube, as shown in Fig. 1. While the temperature of central reaction zone reached

---

[*] Corresponding author at: College of Chemistry and Chemical Engineering, Taiyuan University of Technology, 79, West Yingze Street, Taiyuan 030024, China. Tel./fax: +86 351 6014138.
E-mail address: liuxuguang@tyut.edu.cn (X. Liu).

0022-3697/$ - see front matter © 2009 Elsevier Ltd. All rights reserved.
doi:10.1016/j.jpcs.2009.11.012

predetermined temperature in Ar atmosphere, reaction was allowed to proceed for 30 min by moving the quartz boat into low temperature zone (500–600 °C) near the inlet of the quartz tube, where the pyrolytic gases of DOA were carried into reaction zone by Ar flow. Then the quartz tube was cooled to room temperature under the protection of flowing Ar. Finally, the black powder was collected from high temperature zone (denoted as Zone A in Fig. 1) and low temperature zone near the outlet of the quartz tube (denoted as Zone B in Fig. 1).

Table 1
Analytical data of DOA.

Elemental analysis (wt%)				H/C (mol mol^{-1})	Softening point (°C)	Carbon residue (wt%)
C	H	N	S			
87.84	9.39	1.28	0.42	1.28	193	41.08

Table 2
Main compositions of pyrolytic gases of DOA.

Composition	H_2	N_2	CH_4	CO	CO_2	C_nH_m
Vol%	4.92	37.58	30.43	3.52	2.43	17.32

2.2. Preparation of GCMSs

The CMSs obtained in Section 2.1 were further treated by vacuum heat treatment. Experimental parameters were as follows: vacuum was between 2×10^{-2} and 2×10^{-3} Pa, the vacuum furnace was heated to 2000 °C at the rate of 30 °C/min, kept for 1 h and then cooled to room temperature.

2.3. Modification of CMSs and GCMSs

Air oxidation was performed to modify as-synthesized CMSs. The process parameters and procedures were as follows: 50 mg of CMSs was placed in a small quartz boat and then heated in open air in a horizontal tubular furnace at 500 °C for 1, 2, 3, 5, 7 or 10 h. GCMSs were also oxidized in air at 500 °C for 5 h.

2.4. Characterization

The products were characterized using field emission scanning electron microscope (FESEM, JSM-6700F, operated at 10 kV) equipped with an energy dispersive X-ray spectroscope (EDS), high-resolution transmission electron microscope (HRTEM, JEM-2010, working at an accelerating voltage of 200 kV), Raman spectrometer (JY-HR800, 532 nm), X-ray powder diffractometer (XRD, D/Max-3C, Cu-K$_\alpha$ radiation, λ=1.54018 Å). Functional groups were characterized using Fourier transformation infra-red spectrometer (FTIR, FTS-165).

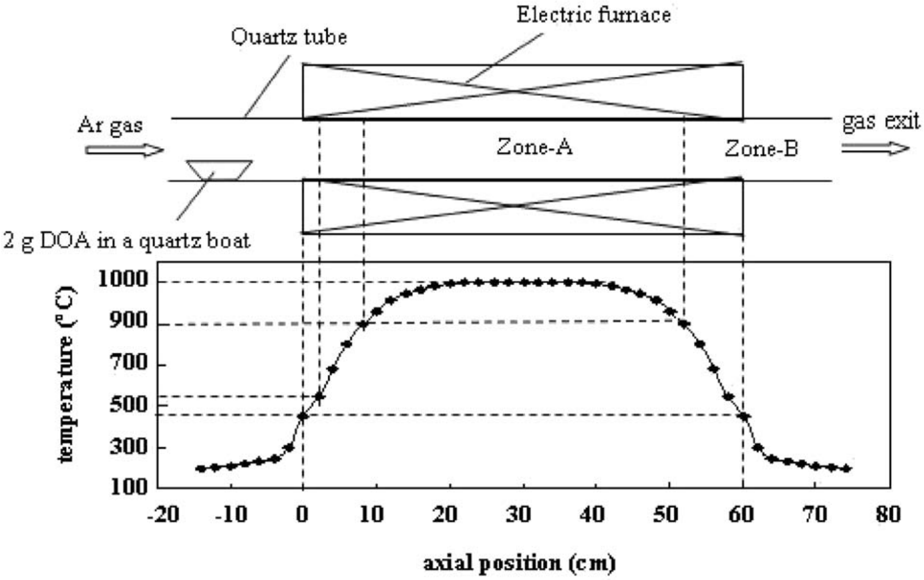

Fig. 1. Schematic of experimental apparatus and the temperature profile along the quartz tube with the central temperature of 1100 °C.

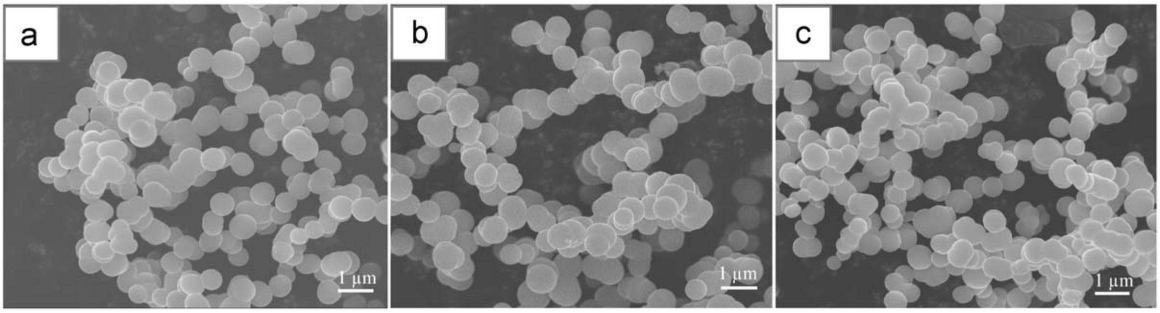

Fig. 2. FESEM images of CMSs obtained at (a) 900, (b) 1000 and (c) 1100 °C.

3. Results and discussion

3.1. Controllable synthesis of CMSs

Fig. 2 shows typical FESEM images of CMSs obtained at different reaction temperatures with Ar flow rate of 180 ml/min and reaction time of 30 min. The diameters of CMSs, distributed in the range of 650–750 nm, were basically invariable with increasing reaction temperature from 900 to 1100 °C. This was consistent with the results of Jin et al. [12]. On the other hand, the yield increased obviously with increasing temperature, as shown in Table 3. The corresponding size distribution and yield data are also listed in Table 3.

Table 3
Effects of the reaction temperatures on the size and yield of CMSs.

No.	Temperature (°C)	Ar flow rate (ml/min)	Reaction time (min)	Size distribution (nm)	Yield [a] (%)
1	900	180	30	650–750	21
2	1000	180	30	650–750	33.6
3	1100	180	30	650–750	35.6

[a] Yield = total mass of CMSs/mass of (raw materials − residue in boat) × 100%.

Table 4
Effects of Ar flow rate on the size and yield of CMSs.

No.	Temperature (°C)	Ar flow rate (ml/min)	Reaction time (min)	Size distribution (nm)	Yield [a] (%)
1	1100	60	30	900–1000	44.7
2	1100	120	30	800–900	41.7
3	1100	180	30	650–750	35.6
4	1100	300	30	200–300	30.7

[a] Yield = total mass of CMSs/mass of (raw materials − residue in boat) × 100%.

Ar flow rate determined the retention time of pyrolytic gases in reaction zone. Therefore, the effect of Ar flow rate on yield and diameters of CMSs was investigated by fixing reaction temperature at 1100 °C and reaction time at 30 min (shown in Table 4). A group of FESEM images are shown in Fig. 3, and the relationship between Ar flow rate and CMSs yield can be found in Table 4. The CMSs obtained at different Ar flow rates were uniform in size. With increasing Ar flow rate from 60 to 300 ml/min, the size of CMSs decreased from 1 µm to 220 nm (shown in Fig. 3) and the yield of CMSs decreased from 44.7% to 30.7% (shown in Table 4). In addition, CMSs obtained at Ar flow rate of 300 ml/min was analyzed by EDS. In the as-prepared samples of CMSs, only carbon was observed (see inset in Fig. 3(c)). It is clear that Ar flow rate played an important role for the formation of CMSs. At lower Ar flow rate, the higher concentration of carbon species formed by decomposition of pyrolytic gases and longer retention time favored the rapid growth of CMSs with subsequent higher yield and larger size. On the other hand, as Ar flow rate got higher, the lower concentration and shorter retention time of carbon species in reaction zone resulted in lower yield and smaller size.

The products above-discussed were collected in high temperature zone (Zone A in Fig. 1). The effect of collection zone was also noticed in this paper. Fig. 4 shows the FESEM images of CMSs obtained in different collection zones with the experimental temperature of 1100 °C, reaction time of 30 min and Ar flow rate of 180 ml/min. As can be seen from Fig. 4, the products obtained in low temperature zone (200–900 °C, Zone B in Fig. 1) were CMSs

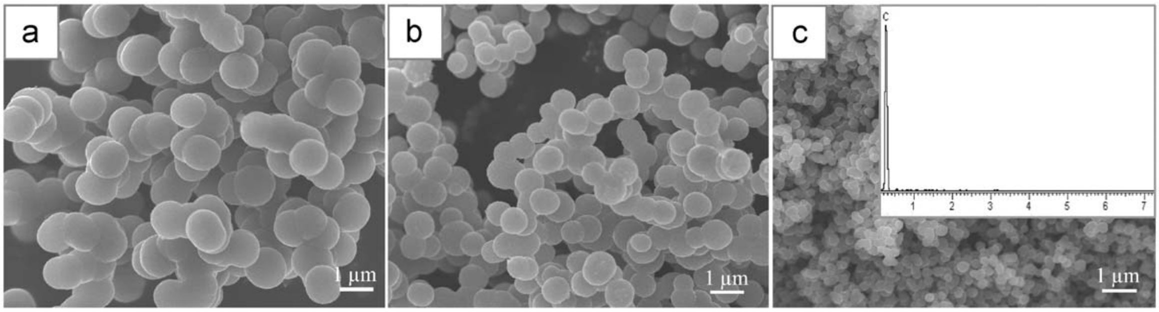

Fig. 3. FESEM images of CMSs obtained at different Ar flow rates: (a) 60, (b) 120, and (c) 300 ml/min (inset in (c) shows EDS patterns of CMSs).

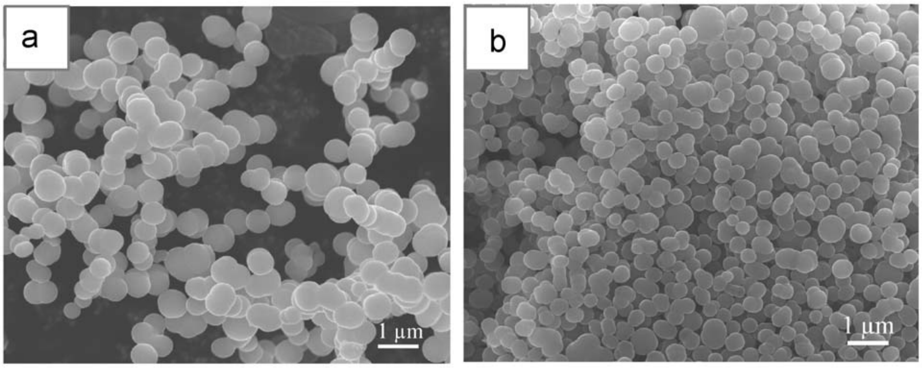

Fig. 4. FESEM images of CMSs collected in (a) high and (b) low temperature zones. Reaction temperature: 1100 °C, time: 30 min, Ar flow rate: 180 ml/min.

with size ranging from 250 to 400 nm, which were smaller than those obtained in high temperature zone (900–1100 °C, Zone A) with size ranging from 650 to 750 nm. During deposition process, some pyrolytic carbon species were carried into Zone B by Ar flow, depositing on the tube wall and resulting in the formation of CMSs with small diameters.

CMSs with different sizes have potential applications because of their excellent properties. A large number of experiments were conducted to synthesize a series of size-controllable and high-quality CMSs from DOA. The experimental results were shown in Table 5 and Fig. 5, and the histograms of size distribution of CMSs were shown in the upper-right-hand corner of the corresponding FESEM images in Fig. 5. By selection of preparation parameters, CMSs with size ranging from 100 nm to 1 μm were synthesized with good size controllability.

Table 5
A series of size-controllable and high quality CMSs.

No.	Experimental parameters	Collection zone	Diameter (nm)	Fig.
1	1100 °C, 30 min, Ar 60 ml/min	Zone A	900–1000	5(a)
2	1000 °C, 30 min, Ar 150 ml/min	Zone A	750–900	5(b)
3	1100 °C, 30 min, Ar 180ml/min	Zone A	650–750	5(c)
4	1100 °C, 20 min, Ar 60 ml/min	Zone B	450–600	5(d)
5	1000 °C, 10 min, Ar 120 ml/min	Zone B	400–550	5(e)
6	1000 °C, 20 min, Ar 180 ml/min	Zone B	300–400	5(f)
7	1100 °C, 30 min, Ar 300 ml/min	Zone A	200–300	5(g)
8	1000 °C, 30 min, Ar 300 ml/min	Zone B	100–200	5(h)

3.2. *Microstructure analysis of CMSs and GCMSs*

Fig. 6(a) and (b) show TEM images of CMSs obtained in 300 ml/min Ar atmosphere at 1100 °C for 30 min, and Fig. 6(c) and (d) show TEM images of GCMSs. Perfect spherical shapes with uniform size and smooth surface can be seen in Fig. 5a, which is consistent with FESEM observation. As shown in Fig. 6(b), CMSs were of low graphitization degree, with discernible graphite layers. The graphitization degree of GCMSs was enhanced, and the graphite layers with space of 0.343 nm was clear (as shown in Fig. 6(d)).

The graphitization degrees of CMSs and GCMSs were also examined by XRD and Raman spectroscopy. Typical XRD patterns of CMSs and GCMSs are shown in Fig. 7. The broad peak at 25.45° (Fig. 7(a)) and the sharp one at 25.9° (Fig. 7(b)) were attributed to the (0 0 2) plane of graphite, and the corresponding d values were

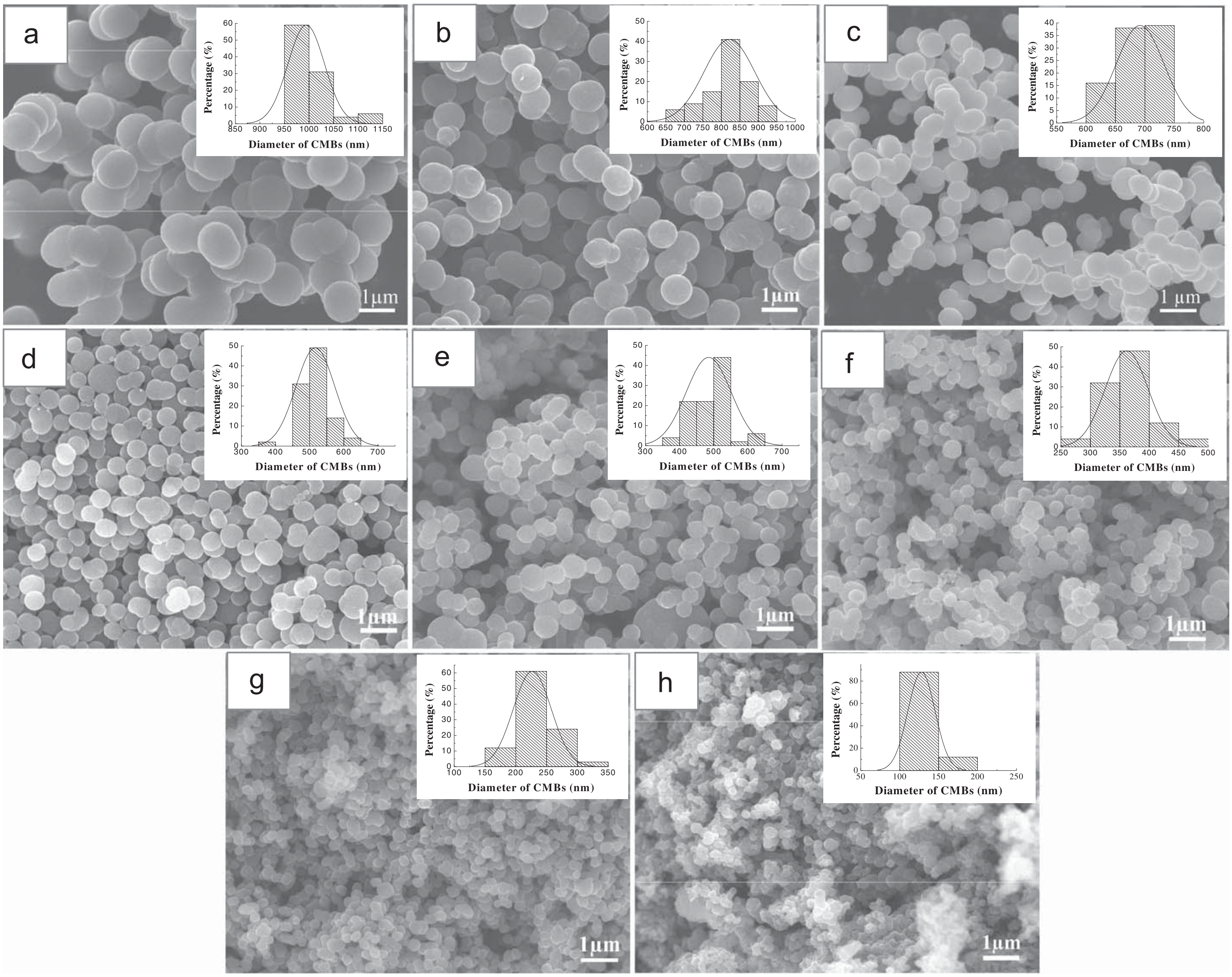

Fig. 5. FESEM images and size distribution histograms (insets) of size-controllable CMSs. Preparation parameters are listed in Table 5.

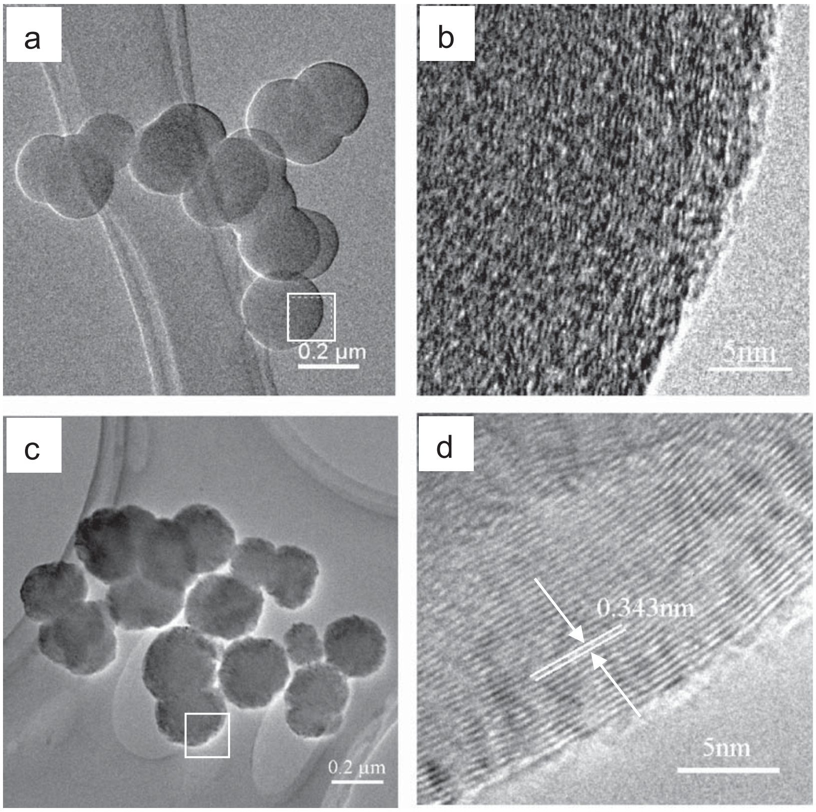

Fig. 6. TEM images of (a) CMSs and (c) GCMSs. (b) and (d) are HRTEM images of the square areas in (a) and (c), respectively.

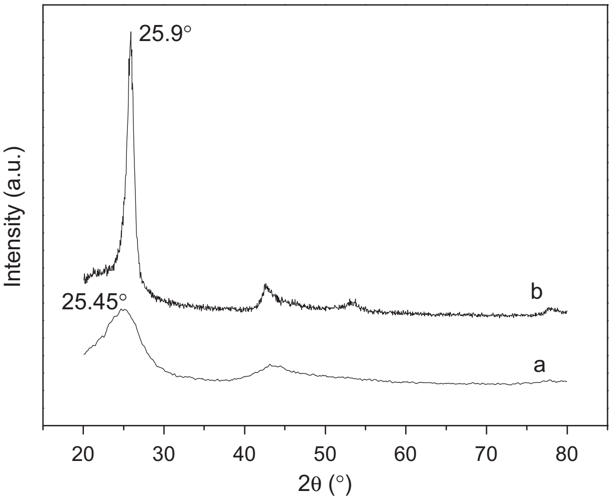

Fig. 7. XRD patterns of (a) CMSs and (b) GCMSs. Preparation parameters for CMSs: temperature: 1100 °C, time: 30 min, Ar flow rate: 300 ml/min. Preparation parameters for GCMSs: vacuum heat treatment at 2000 °C for 1 h.

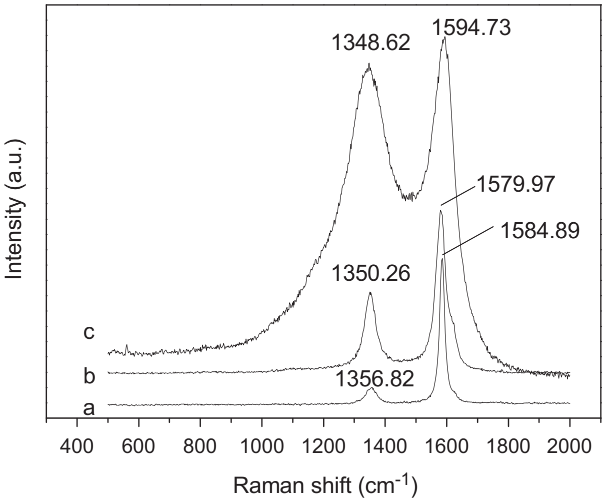

Fig. 8. Raman spectra of (a) graphite, (b) GCMSs and (c) CMSs. Preparation parameters for CMSs and GCMS (see Fig. 7).

0.349 and 0.343 nm, respectively. This suggests that the graphitization degree of GCMSs was largely enhanced after vacuum heat treatment. Fig. 8 shows Raman spectra of graphite, GCMSs and CMSs. In the Raman spectra, G band was attributed to the stretching modes of C–C bonds of typical graphite, while D band was related to the defects and disordered carbonaceous solid. The D bands of graphite, GCMSs and CMSs were observed at 1356.82, 1350.26 and 1348.62 cm^{-1}, respectively, as shown in Fig. 8. The I_G/I_D values of graphite, GCMSs and CMSs were 5.172, 1.853 and 1.074, respectively, implying that the graphitization degree of CMSs was improved by vacuum heat treatment, in good agreement with HRTEM and XRD results.

3.3. *Modification of CMSs and GCMSs*

FTIR spectra were used to investigate the residual functional groups on the surface of GCMSs and CMSs after oxidation in air for different times, as shown in Figs. 9 and 10. The assignments of absorption bands are listed in Table 6.

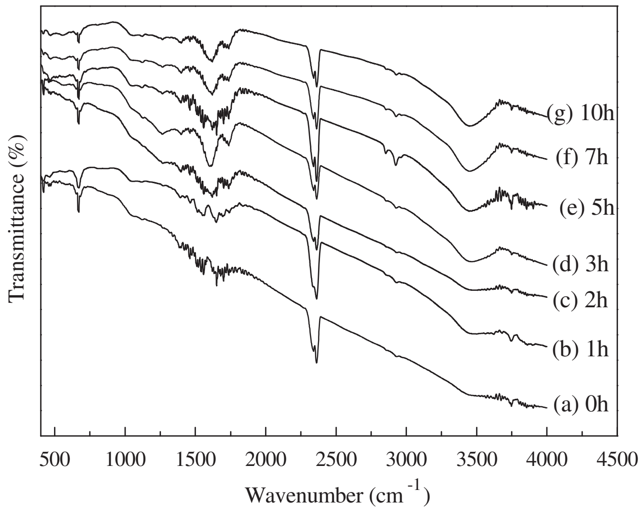

Fig. 9. FTIR spectra of the CMSs oxidized in air for different times.

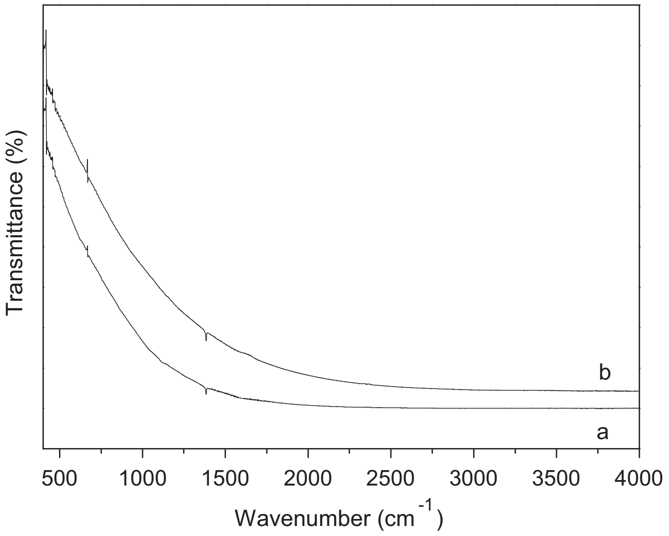

Fig. 10. FTIR spectra of (a) as-prepared GCMSs and (b) GCMSs oxidized in air for 5 h.

The FTIR spectra of CMSs oxidized in air for 1 h (Fig. 9(b)) was similar to original sample (Fig. 9(a)), indicating that no new functional groups were introduced onto the surface of CMSs when oxidation time was less than 1 h. With the oxidation time being increased to 2 h, two relatively weak peaks were observed at 1593 and 1701 cm^{-1} (Fig. 9(c)), corresponding to anion carboxylate and carboxylic group, respectively. When the oxidation went on for 3 h, the intensity of anion carboxylate (1613 cm^{-1}) and carboxylic group (1738 cm^{-1}) became stronger and a new peak attributed to hydroxyl group was observed at 3465 cm^{-1} (Fig. 9(d)). When the CMSs were oxidized for 5, 7 and 10 h (Fig. 9(e–g)), the peaks of carboxylate and carboxylic groups were all observed at 1620 and 1738 cm^{-1}, respectively; however, red shift was observed for hydroxyl group at 3464, 3450 and 3450 cm^{-1}. It seems that free hydroxyl groups became associated among different molecules with increasing oxidation time.

In Fig. 10, almost no functional groups appear on the surface of as-prepared and air-oxidized GCMSs. We assumed that vacuum heat treatment at high temperature substantively eliminated the dangling bonds on the surface of GCMSs, so no detectable amount of functional groups were grafted on the highly graphitized surface of GCMSs.

Table 6
Observed FTIR bands for CMSs and their assignments.

Band (cm^{-1})	Assignment
~1620	Carboxylate asymmetric stretching
~1738	C–O stretching
~2362	O–C–O stretching
2854, 2924	C–H stretching
~3400	O–H stretching

This experiment reveals that there were some functional groups such as carboxylate, carboxylic groups and hydroxyl group presented on the surface of CMSs, which would facilitate the grafting of biomolecules or catalytic species onto the surface.

4. Conclusion

In brief, size-controllable CMSs were synthesized from DOA by CVD, with emphasis on the effects of reaction temperature, Ar flow rate and collection zone. GCMSs were obtained from as-prepared CMSs by vacuum heat treatment at 2000 °C for 1 h. Results show that an effective mass production of size-controllable CMSs, with diameters ranging from 100 nm to 1 μm, was proposed. With the reaction temperature being increased from 900 to 1100 °C, the diameters of CMSs distributed in the range of 650–750 nm and the yield increased obviously. With increasing Ar flow rate from 60 to 300 ml/min, the sizes of CMSs decreased from 1 μm to 220 nm, and the yield of CMSs also decreased. The products collected in low temperature zone were CMSs with smaller size and broader size distribution than that obtained in high temperature zone. The graphitization degree of GCMSs was enhanced obviously after vacuum heat treatment. In addition, air oxidation was performed to realize the surface modification of CMSs. FTIR spectra indicated the existence of some oxygen-containing functional groups, including anion carboxylate, carboxylic group and hydroxyl group, on the surface of CMSs oxidized in the air for different times. On the other hand, no functional groups were introduced onto the surface of GCMSs by air oxidization.

Acknowledgements

The authors acknowledge financial support from National Nature Science Foundation of China (20676086), Natural Science Foundation of Shanxi Province (2009011012-4), Program for New Century Excellent Talent in University (NCET-06-0262), International S&T Co-operation Program (2007DFA50940), Shanxi Research Fund for Returned Scholars (2008-31) and Taiyuan S&T Program (08121024).

References

[1] D. Ugarte, Curling and closure of graphitic networks under electron-beam irradiation, Nature 359 (1992) 707–709.
[2] S. Iijima, Helical microtubules of graphitic carbon, Nature 354 (1991) 56–58.
[3] Y.Z. Jin, Y.J. Kim, C. Gao, Y.Q. Zhu, A. Huczko, M. Endo, H.W. Kroto, High temperature annealing effects on carbon spheres and their applications as anode materials in Li-ion secondary battery, Carbon 44 (2006) 724–729.
[4] Z.F. Wang, P.F. Xiao, N.Y. He, Synthesis and characteristics of carbon encapsulated magnetic nanoparticles produced by a hydrothermal reaction, Carbon 44 (2006) 3277–3284.
[5] S.I. Lee, S. Mitani, C.W. Park, S.H. Yoon, Y. Korai, I. Mochida, Electric double-layer capacitance of microporous carbon nano spheres prepared through precipitation of aromatic resin pitch, J. Power Source 139 (2005) 379–383.

[6] N. Liu, S.T. Zhang, R.W. Fu, M.S. Dresselhaus, G. Dresselhaus, Carbon aerogel spheres prepared via alcohol supercritical drying, Carbon 44 (2006) 2430–2436.

[7] M. Kodama, T. Fujiura, E. Ikawa, K. Esumi, K. Meguro, H. Honda, Characterization of meso-carbon microbeads prepared by emulsion method, Carbon 29 (1991) 43–49.

[8] Y.G. Lu, L.C. Ling, S. Oh, Y. Park, Preparation of carbon microbeads from pitch and resin by suspension, New Carbon Mater. 16 (2001) 1–5.

[9] J.W. Liu, M.W. Shao, Q. Tang, X.Y. Chen, Z.P. Liu, Y.T. Qian, A medial-reduction route to hollow carbon spheres, Carbon 41 (2002) 1682–1685.

[10] J.S. Qiu, Y.F. Li, Y.P. Wang, C.H. Liang, T.H. Wang, D.H. Wang, A novel form of carbon micro-balls from coal, Carbon 41 (2003) 767–772.

[11] H.S. Qian, F.M. Han, B. Zhang, Y.C. Guo, J. Yue, B.X. Peng, Non-catalytic CVD preparation of carbon spheres with a specific size, Carbon 42 (2004) 761–776.

[12] Y.Z. Jin, C. Gao, W.K. Hsu, Y.Q. Zhu, A. Huczko, M. Bystrzejewski, M. Roe, C.Y. Lee, S. Acquah, H. Kroto, D. Walton, Large scale synthesis and characterization of carbon spheres prepared by direct pyrolysis of hydrocarbons, Carbon 43 (2005) 1944–1953.

[13] A.L. Ma, X.M. Wang, T.B. Li, X.G. Liu, B.S. Xu, Characteristics of carbon microspheres and study on its adsorption isotherms, Mater. Sci. Eng. A-Struct. 443 (2007) 54–59.

[14] X.G. Liu, Y.Z. Yang, X. Lin, B.S. Xu, Y. Zhang, Deoiled asphalt as carbon source for preparation of various carbon materials by chemical vapor deposition, Fuel Process. Technol. 87 (2006) 919–925.

[15] Y.Z. Yang, X.G. Liu, B.S. Xu, T.B. Li, Preparation of vapor grown carbon fibers from deoiled asphalt, Carbon 44 (2006) 1661–1664.

[16] Y.Z. Yang, C.Y. Zhang, W.Y. Ji, X.G. Liu, B.S. Xu, Synthesis of iron-containing carbon particles from deoiled asphalt and ferrocene, Chin. J. Aeronaut. 19 (2006) S228–S231.

[17] B.S. Xu, C.Y. Zhang, Y.Z. Yang, X.G. Liu, Q.P. Luo, $FeCl_3$-catalyzed growth of vapor-grown carbon fibers from deoiled asphalt, New Carbon Mater. 22 (2007) 1–6.

[18] X.G. Liu, Y.Z. Yang, H.Y. Liu, W.Y. Ji, C.Y. Zhang, B.S. Xu, Carbon nanotubes from catalytic pyrolysis of deoiled asphalt, Mater. Lett. 61 (2007) 3916–3919.

[19] Y.Z. Yang, X.G. Liu, B.S. Xu, Fe-encapsulating carbon nano onion-like fullerenes from heavy oil residue, J. Mater. Res. 23 (2008) 1393–1397.